FINAL REPORT

A COMPUTER-BASED DESIGN OF NEW OZONE CONTACTOR TREATING PALDANG DAM RESERVOIR WATER

Prepared by

Dooil Kim
Graduate Research Assistant
Environmental Engineering Program
School of Civil and Environmental Engineering
Georgia Institute of Technology
Atlanta, GA 30332-0512
E-mail: gtg722i@mail.gatech.edu

And

Jae-Hong Kim, Ph.D.
Assistant Professor
Environmental Engineering Program
School of Civil and Environmental Engineering
Georgia Institute of Technology
Atlanta, GA 30332-0512
Phone: 404-894-2216
Fax: 404-894-8266
E-mail: jaehong.kim@ce.gatech.edu

For

Myung Hoon Jang, Ph.D.
President
Shinwoo Engineering Co., LTD.
5442-1Sangdaewon-Dong, Jungwon-Gu, Seonam-Si, Kyonggi-Do, Korea
Tel: 82-2-572-2211
Fax: 82-31-736-0308

September 1, 2005

CONTENTS

1. INTRODUCTION

1.1 Ozone Disinfection Processes

A chemical disinfection process is one of the key unit operations in water treatment processes to inactivate pathogenic microorganisms and to ensure biological safety of potable water. Typical disinfectants used for drinking water treatment include chlorine, chlorine dioxide, chloramines and ozone. Among these chemicals, ozone has been receiving the most attention since the outbreak of *Cryptosporidium parvum* oocysts in 1993 in Milwaukee, WI (Smith, 1995). Although the operational costs of ozone disinfection process are relatively higher than chlorine-based treatment processes in general, ozone is the most effective disinfectant against *C. parvum* oocyst (Kolich et al., 1990; Gyűrék et al., 1997; Rennecker et al., 1999, 2000, 2001; Driedger et al., 2000, 2001). In comparison to chlorine-based processes, ozonation has also been shown to produce much lower levels of chlorinated disinfection by-products such as trihalomethanes (THMs) and haloacatic acids (HAAs). Control of taste and odor causing compounds and oxidation of ferrous iron and manganese have been additional treatment goals (Langlais et al., 1991). Ozonation typically increases biodegradability of natural organic matter. Therefore, a subsequent filtration with biologically activated carbon has been recognized as a standard method to remove organic matter that is capable of promoting microbial re-growth in the distribution network (van der Kooji et al., 1992; Volk et al., 2002).

1.2 Computer Model and Numerical Simulation

Pilot studies have often been employed to determine key design and operational parameters for a new ozone reactor as well as to upgrade and optimize existing ozone treatment facilities. Unfortunately, pilot studies are often time-consuming and labor and cost extensive. In addition, extrapolating the pilot-scale results to the design of full-scale treatment facilities has not always been straightforward. As an alternative to pilot-scale studies, mathematical modeling and numerical simulation have been suggested by several researchers. Sophisticated steady-state and dynamic computer models might greatly simplify the tasks of understanding physical, chemical, and biological processes in ozonation processes. The mathematical modeling might

further allow a prediction of reactor performances under a wide spectrum of configurational and operational scenarios. Accordingly, the *OCM* (Ozone Contactor Model) is the software developed by Georgia Institute of Technology, University of Illinois at Urbana-Champaign, and US Environmental Protection Agency with the goal of performing complex simulation tasks in designing and optimizing ozone bubble-diffuser contactors. The applicability of the *OCM* has recently been verified by full-scale experiments with two existing ozone contactors in the US (Tang et al., 2005; Kim et al. 2005).

1.3 Research Objectives

The objectives of this research were: 1) to determine ozone decay and bromate formation kinetic constants in raw waters collected from Banwal Water Treatment Plants (BWTP), Ansan, Korea, at different pHs and temperatures; 2) to simulate ozone and bromate concentrations and *C. parvum* oocyst inactivation in an existing full-scale ozone contactor in the BWTP using the *OCM* software at different pHs and temperatures using the kinetics determined from the batch tests; and 3) to evaluate alternative design options such as the number of cell divisions and hydrodynamic conditions (i.e., expressed in dispersion numbers).

2. MATERIAL AND METHODS

2.1 Ozone Decay Kinetic Constants Measurement

A water sample was collected from the filter effluent of the BWTP on April 1, 2005 and transported to Georgia Institute of Technology in a refrigerated container via express delivery. Ozone decay kinetic constants and fast ozone demands were measured using a newly developed multi-channel stopped-flow reactor (MC-SFR) system. Figures 1 and 2 are a schematic diagram and a photograph of MC-SFR system, respectively. The MC-SFR automatically measures ozone decay kinetics. The details of MC-SFR setup and experimental procedures are described elsewhere (Kim and Kim, 2004).

2.2 Bromate Formation Kinetic Constant Measurements

The MC-SFR also serves as a batch reactor to determine bromate formation kinetics. For bromate concentration analysis, 2-3 mL of samples were collected from the outlet of the MC-SFR system and instantaneously mixed with 0.1 mL of 0.5 M ethylenediamine (EDA) solution to quench the residual ozone. Concentrations of bromate and bromide ions were measured according to EPA method 317.0 (USEPA, 2001) using a Dionex DX-600 ion chromatography system (Dionex, Sunnyvale, CA). The measurement apparatus was composed of AS50 (Auto sampler and Chromatography compartment), GP50 (Gradient pump), ED50 (Electrochemical detector), Ionpac AS90-HC (4×250mm) column, AG9-HC (4×50mm) guard column, Anion Atlas suppressor.

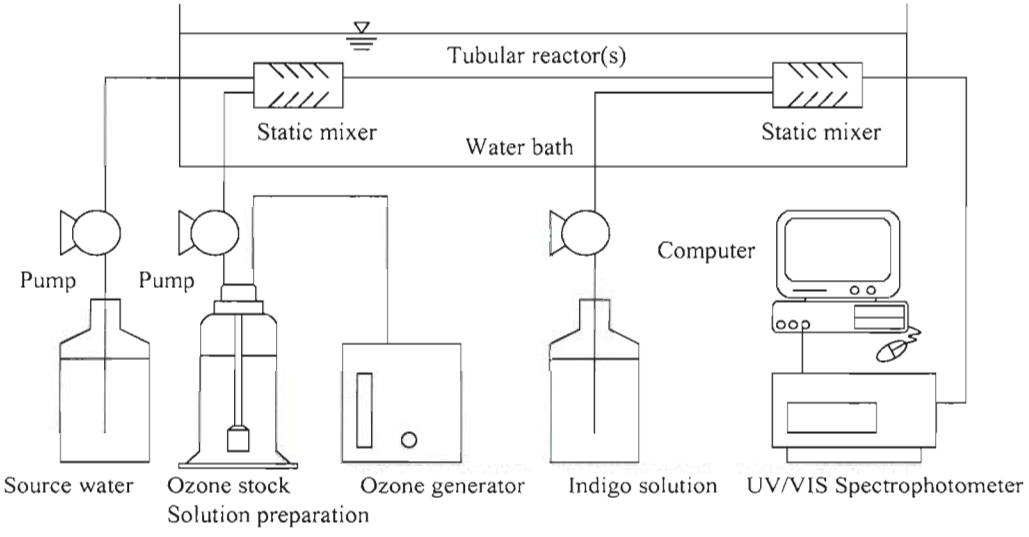

Figure 1. A schematic representation of the Multi-Channel Stopped Flow Reactor (MC-SFR).

2.3 Miscellaneous Analyses

Total organic carbon (TOC) was measured using a TOC-Vws wet oxidation TOC analyzer (Shimazu, Kyoto, Japan) based on a non-purgeable organic carbon (NPOC) method. UV_{254} was measured using an Agilent 8453 spectrophotometer (Agilent, Palo Alto, CA, USA). Specific UV absorbance (SUVA) was calculated by dividing UV_{254} (1/cm) absorbance by TOC

(mg/L). pH and turbidity were measured using an Accumet AR-50 pH meter (Fisher Scientific, Pittsburg, PA, USA) and Hach 2100N turbidometer (Hach, Loveland, CO, USA), respectively.

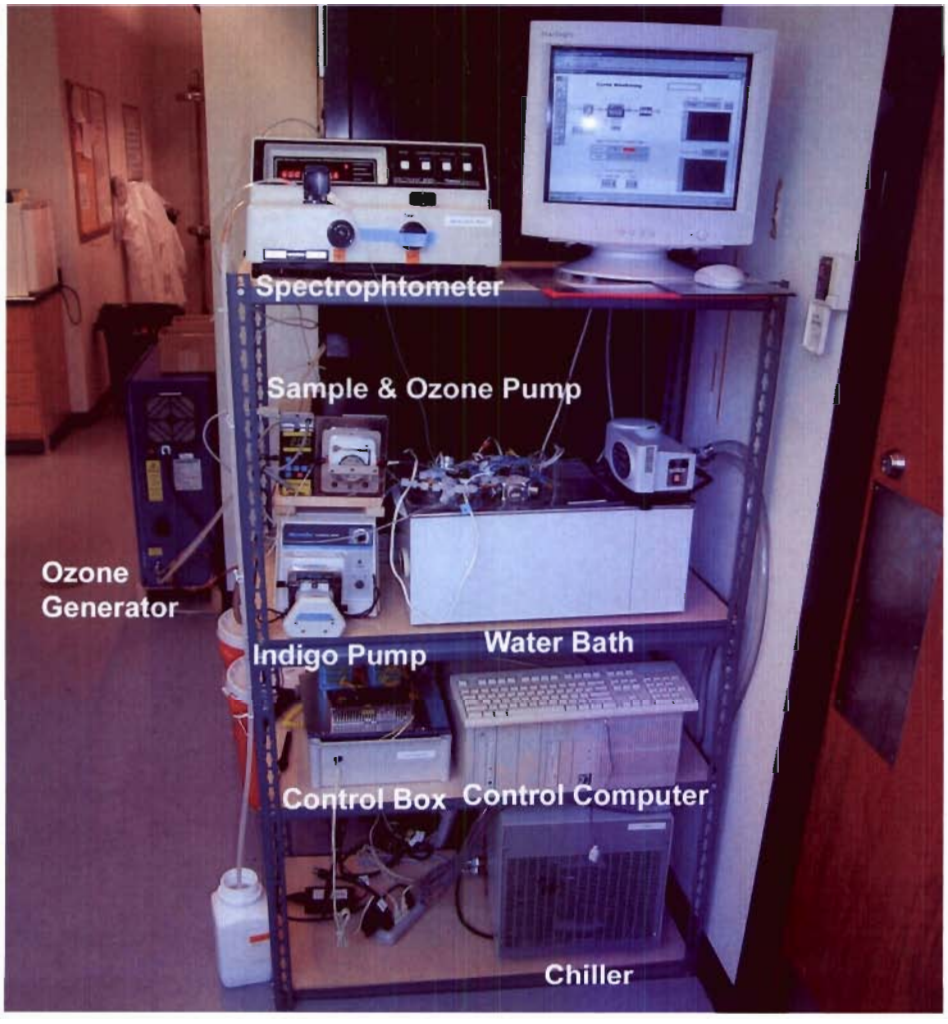

Figure 2. A photograph of the MC-SFR system. The tubular reactors are contained inside a water bath shown in the photograph.

2.4 BWTP (Banwal Water Treatment Plant)

The treatment process in the BWTP consists of coagulation/flocculation/sedimentation, sand filtration, ozonation, biologically activated carbon filtration, and secondary disinfection as shown in Figure 3. The BWTP has two ozone contactors with a design volume of 1,914.1 m^3 (18.0 m W × 18.2 m L × 6.0 m H). The design flow rate to each ozone contactor is 183,751 m^3/d

with an average hydraulic retention time of 15.4 min. Ozone is injected by a side stream injector at the inlet of the ozone contactors.

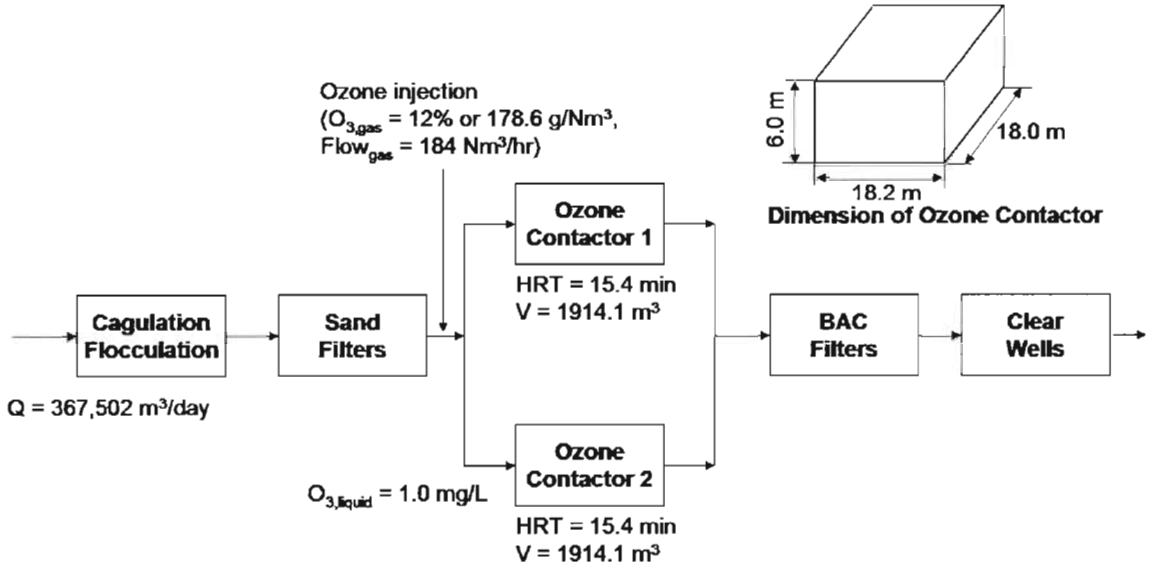

Figure 3. A schematic diagram of the BWTP with relevant dimensions and flow rates.

2.5 *OCM* : Ozone Contactor Simulation Software

The *OCM* has the capability of simultaneously predicting steady-state residual ozone concentration, *C. parvum* oocyst inactivation, and bromate formation in a multi-chamber ozone bubble-diffuser contactors (i.e., number of cells from 1 to 20). The simulation results are given as the profiles across the ozone contactor. The *OCM* is targeted for the engineers involved in the design and operation of ozone disinfection systems, plant operators responsible for optimizing system operation and demonstrating regulatory compliance, and government officials in charge of developing drinking water regulations, who are not necessarily familiar with formulations and numerical analyses involved in these mathematical models. Therefore, the *OCM* was designed to work on a personal computer equipped with a commonly available operating system, Microsoft Windows® (i.e., Windows 2000® or higher version) and to provide graphical user interfaces that are familiar to Windows users.

The hydrodynamic and reaction parameters formulated by the equations are listed in Table 1. The equations were solved for each chamber of ozone contactor assuming ideal closed vessel boundary conditions (Kim *et al.*, 2002a, 2005b) at each boundary between adjacent chambers. The boundary conditions are summarized in Table 2. Figure 4 shows a snapshot of the *OCM* running on Microsoft Windows® XP operating system. Details of the software are available in Kim *et al.* (2005b).

Table 1. Mass balance equations for dissolved ozone, fast ozone demand, gas phase ozone, microorganism, and bromate, which are solved by the *OCM* software. For definitions of terms used, refer to Kim et al. (2005b).

Dissolved ozone

$$E_L \cdot \frac{d^2[O_3]_l}{dx^2} \mp U_L \frac{d[O_3]_l}{dx} + k_L a \cdot \left(\frac{[O_3]_g}{m} - [O_3]_l \right) - k_d \cdot [O_3]_l - k_R \cdot [O_3]_l \cdot [D] = 0 \quad (1)$$

Fast ozone demand

$$E_L \cdot \frac{d^2[D]}{dx^2} \mp U_L \frac{d[D]}{dx} - k_R \cdot [O_3]_l \cdot [D] = 0 \quad (2)$$

Gas phase ozone

$$U_G \frac{d[O_3]_g}{dx} - k_L a \cdot \left(\frac{[O_3]_g}{m} - [O_3]_l \right) = 0 \quad (3)$$

C. parvum oocyst

$$E_L \cdot \frac{d^2 N}{dx^2} \mp U_L \frac{dN}{dx} - k_N \cdot N \cdot [O_3]_l = 0 \quad (4)$$

Bromate

$$E_L \cdot \frac{d^2[BrO_3^-]}{dx^2} \mp U_L \frac{d[BrO_3^-]}{dx} + k_{BrO3^-} \cdot [O_3]_l = 0 \quad (5)$$

$[O_3]_l$ = dissolved ozone concentration [ML^{-3}]; [D] = fast ozone demand concentration [ML^{-3}]; $[O_3]_g$ = gas phase ozone concentrations [ML^{-3}]; N = number density of viable microorganisms [L^{-3}]; [BrO_3^-] = bromate concentration [ML^{-3}]; E_L = liquid phase dispersion coefficients [L^2T^{-1}]; x = distance from the top of each chamber in the axial direction regardless of liquid flow direction [L]; k_La = volumetric mass transfer coefficient [T^{-1}]; m = Henry's law coefficient

[dimensionless]; k_D = first-order ozone decay rate constant [T^{-1}]; k_R = second order rate constant for ozone reaction with fast ozone demand [$L^3M^{-1}T^{-1}$]; k_N = second-order inactivation rate constant [$L^3M^{-1}T^{-1}$]; k_{BrO3-} = first-order bromate formation rate constant [T^{-1}]; U_L, U_G = liquid and gas phase approach velocities [LT^{-1}]

Table 2. Bounday conditions for the governing equations presented in Table 1. For definitions of terms used, refer to Kim et al. (2005b).

	Counter-current mode		Co-current mode	
Dissolved species	$C\big\|_{z=0} = C_0 + d \cdot \left.\frac{dC}{dx}\right\|_{x=0}$	(6)	$\left.\frac{dC}{dx}\right\|_{x=0} = 0$	(9)
	$\left.\frac{dC}{dx}\right\|_{x=1} = 0$	(7)	$C\big\|_{x=1} = C_0 - d \cdot \left.\frac{dC}{dx}\right\|_{x=1}$	(10)
Gas phase ozone	$[O_3]_g\big\|_{x=1} = [O_3]_{g,0}$	(8)	$[O_3]_g\big\|_{x=1} = [O_3]_{g,0}$	(11)

C = $[O_3]_l$, N, or $[BrO_3^-]$, l = depth of the water column [L]; and $d = E_L/(L \cdot U_L)$ = dispersion number or inverse of Péclet number [dimensionless]

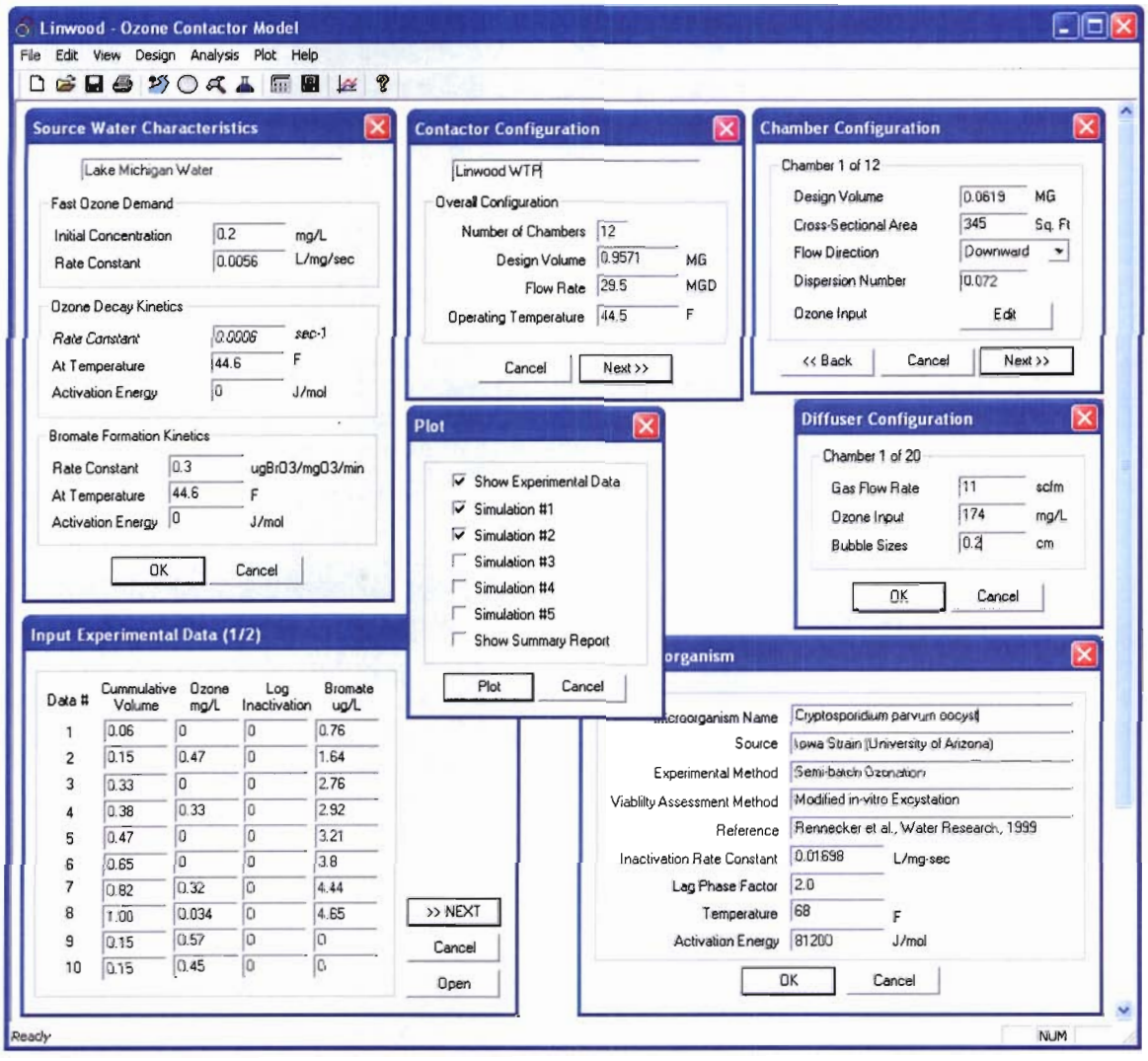

Figure 4. Main window of the *OCM* and various input dialog boxes. (Kim et al., 2005b)

3. RESULTS AND DISCUSSION

3.1 Raw Water Quality

Table 3 shows the water quality parameters for the sample used throughout this study determine using the methods described previously.

Table 3. Water quality parameters measured for the sand filter effluents in the BWTP collected on April 1, 2005.

Br (μg/L)	*pH*	*UV_{254} (1/cm)*	*TOC (mg/l)*	*Turbidity (NTU)*
9.46	6.82	0.0207	1.40	0.419

3.2 Ozone Decay Kinetic Constants

Figures 5, 6, and 7 show the ozone decay kinetics at three different temperatures (i.e., 5, 15, and 25 °C) at pH 6.0, 7.0, and 8.0, respectively. These results were re-plotted in Figures 8, 9, 10 to compare ozone decay at different pHs at the same temperature. Table 4 summarizes ozone kinetic constants and fast ozone demand obtained for each pH and temperature.

Table 4. Ozone decay kinetic constants and fast ozone demand at three different pHs and three different temperature s.

Temp.	pH = 6.0		pH = 7.0		pH = 8.0	
	k_d (1/s)	D_0 (mg/L)	k_d (1/s)	D_0 (mg/L)	k_d (1/s)	D_0 (mg/L)
5 °C	0.00033	0.15	0.00053	0.08	0.00065	0.14
15 °C	0.00047	0.22	0.00090	0.36	0.00101	0.57
25 °C	0.00076	0.46	0.00155	0.65	0.00196	0.83

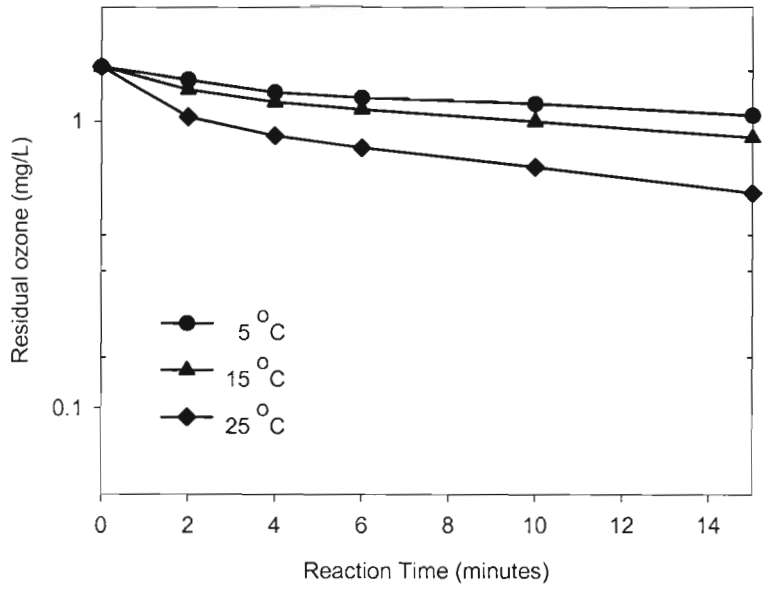

Figure 5. Ozone decay curve in water sample from the BWTP at different temperatures and pH 6.0. $[O_3]_0$ = 1.44 mg/L.

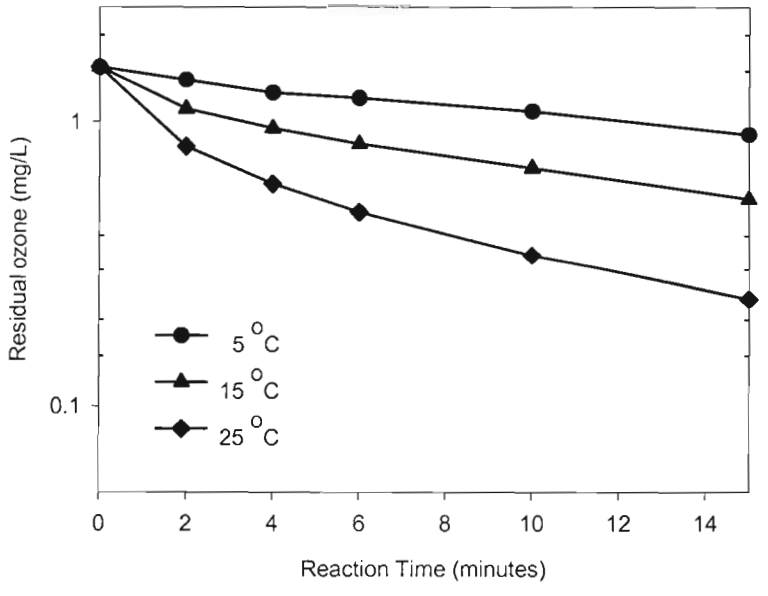

Figure 6. Ozone decay curve in water sample from the BWTP at different temperatures and pH 7.0. $[O_3]_0$ = 1.44 mg/L.

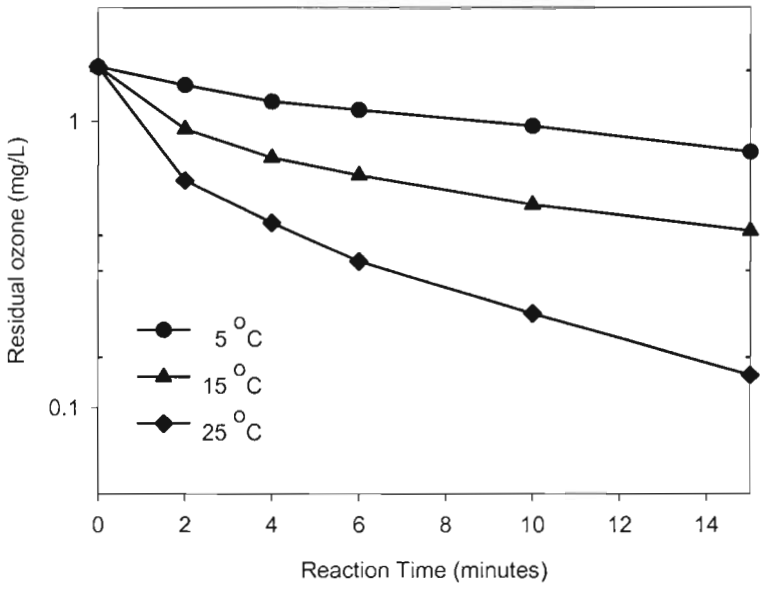

Figure 7. Ozone decay curve in water sample from the BWTP at different temperatures and pH 8.0. $[O_3]_0$ = 1.44 mg/L.

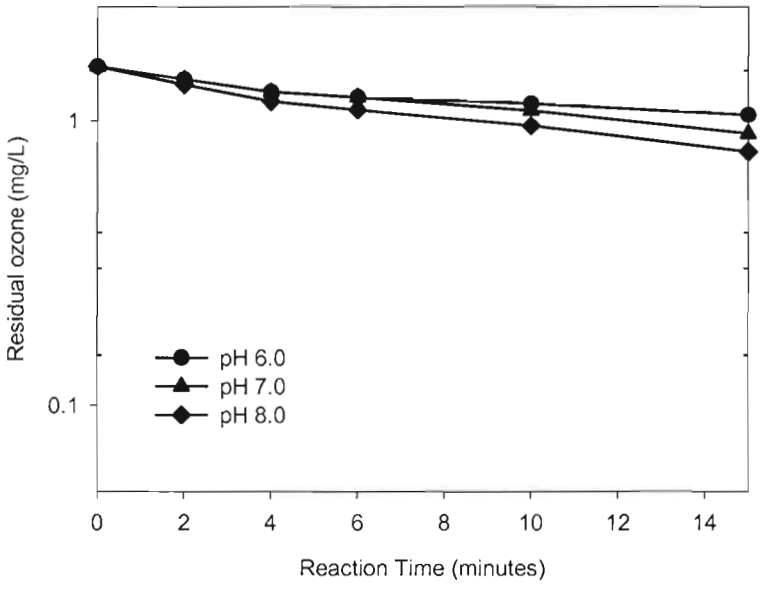

Figure 8. Ozone decay curve in water sample from the BWTP at different pHs and 5 °C. $[O_3]_0$ = 1.44 mg/L.

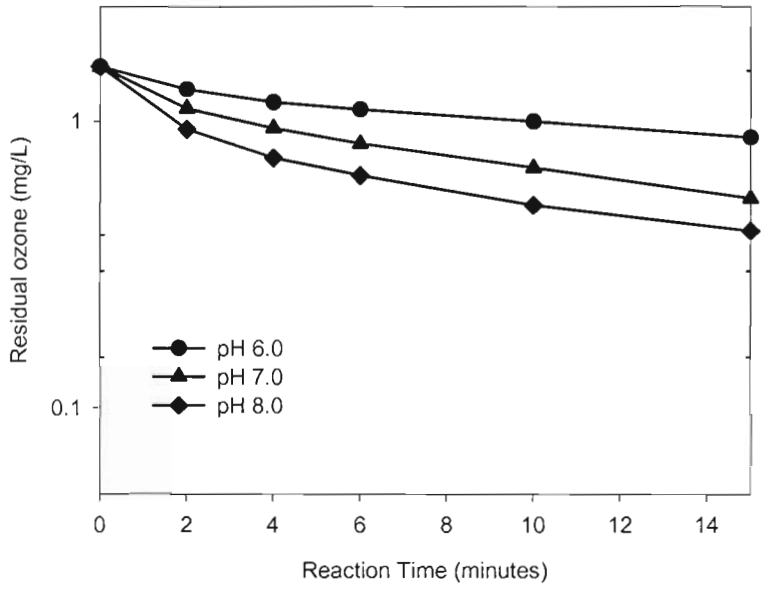

Figure 9. Ozone decay curve in water sample from the BWTP at different pHs and 15 °C. $[O_3]_0$ = 1.44 mg/L.

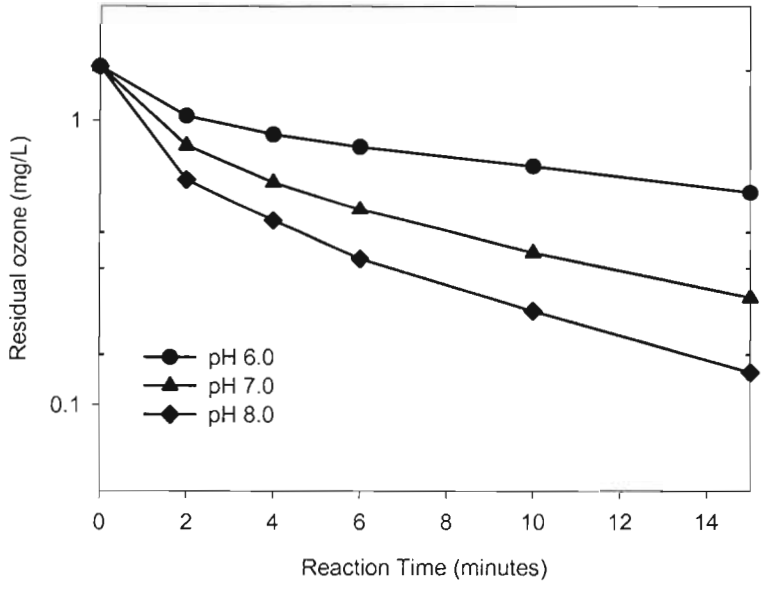

Figure 10. Ozone decay curve in water sample from the BWTP at different pHs and 25 °C. $[O_3]_0$ = 1.44 mg/L.

The observed effect of temperature on the kinetic constants can be mathematically represented using the following Arrhenius expression:

$$k = A \times \exp(-\frac{E_a}{RT}) \qquad [12]$$

in which A is an frequency factor, E_a is an activation energy (J/mol), R is the ideal gas constant, and T is absolute temperature (°K). Figure 11 shows that the observed ozone decay kinetics followed this expression. Activation energy and frequency factor obtained from the slope and y-intercept of these graphs are summarized in Table 5. These results were later used to predict ozone decay rates at different temperatures during full-scale simulation.

Table 5. Activation energy and frequency factors at different pHs.

	pH = 6.0	pH = 7.0	pH = 8.0
E (J/mol)	28308.8	36672.6	37713.9
An	67.4	4111.7	7648.4

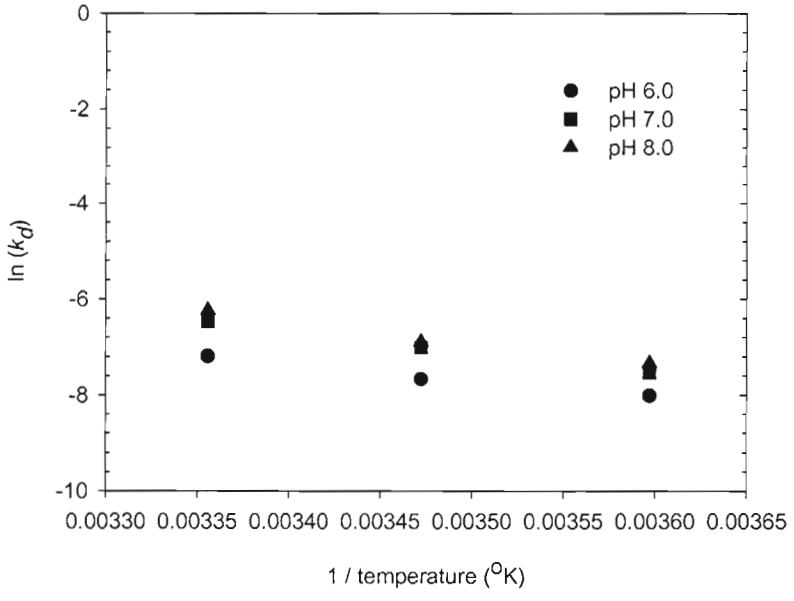

Figure 11. Temperature dependence of ozone decay kinetic rate constants.

3.3 *C. parvum* Inactivation Kinetics

Clark et al. (2002) provided a critical review on the *C. parvum* oocyst inactivation kinetics reported in the literature based on the following Chick-Watson model:

$$ln(N_t / N_0) = -KCt \qquad [13]$$

where N_t and N_0 are the number of viable *C. parvum* oocysts at time t and zero, respectively, and C is the concentration of residual ozone. The effect of temperature on K can be expressed by the following equation.

$$K = 0.118 \times (1.10)^T \qquad [14]$$

This equation was proposed as the best fit to experimental data by Clark et al. (2002) but did not include any safety factor. In contrast, the following equation used in this study estimates K with the 90% confidence interval (Clark et al, 2002).

$$K = 0.06 \times (1.10)^T \qquad [15]$$

3.4 Bromate Formation Kinetics

Kinetics of bromate formation at different temperatures are shown in Figures 12, 13, and 14 at different pHs, respectively. Table 6 summarizes bromate formation kinetics and fast bromete formation constants (i.e., portions of bromate instantaneously formed during the initial stage of ozonation) obtained from analyzing these results. Since the raw water contained a relatively low level of bromide, the bromate formation level was relatively small at less than 3.5 μg/L for all experimental conditions examined (i.e., within 25 mg-min/L of *CT*). Note that this value is much lower than the regulatory level currently set by the EPA in the US (i.e. MCL = 10 μg/L).

It is interesting to note that large quantity of bromate was formed instantaneously, i.e. within 3 mg-min/L of CT regardless of pH and temperature. This indirectly suggests that the major pathway to bromate formation during initial stage of ozonation might be related to oxidation by hydroxyl radical which does not involve hypobromite ions. Note that hypobromite ion (pK_a = 8.8) is a key intermediate in bromate formation by direct oxidation by ozone. Effect of temperature on bromate formation when plotted versus CT was relatively small for all pHs investigated.

Table 6. Bromate formation kinetic constants and amount of initial bromate formation for different pHs and different temperatures. Unit: (μg BrO_3^-/L) / (min·mgO_3/L) for k_{BrO3-} and μg/L for $BrO_3^-{}_{,0}$

Temp.	pH = 6.0		pH = 7.0		pH = 8.0	
	k_{BrO3-}	$BrO_3^-{}_{,0}$	k_{BrO3-}	$BrO_3^-{}_{,0}$	k_{BrO3-}	$BrO_3^-{}_{,0}$
5 °C	0	1.94	0.066	1.58	0.080	1.76
15 °C	0.008	1.68	0.099	1.42	0.111	1.73
25 °C	0.025	1.65	0.100	1.38	0.110	1.87

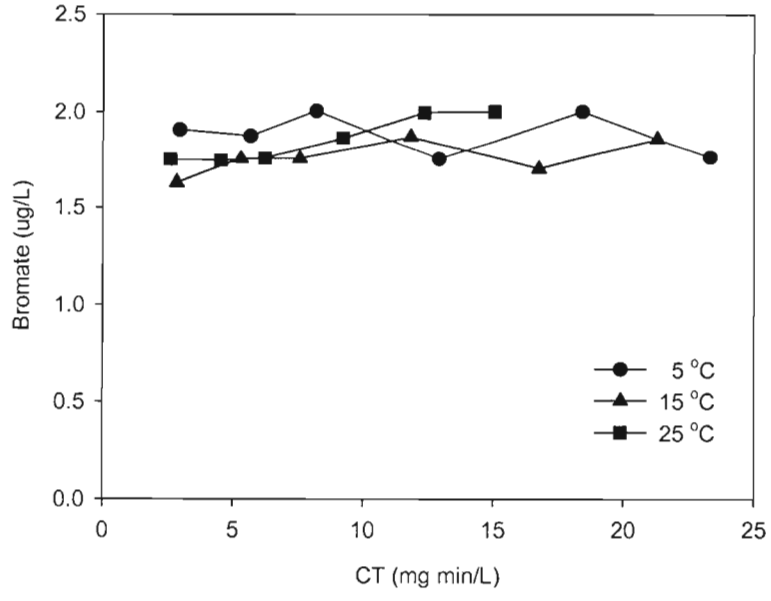

Figure 12. Bromate formation kinetics as a function of CT at different temperatures and pH 6.0.

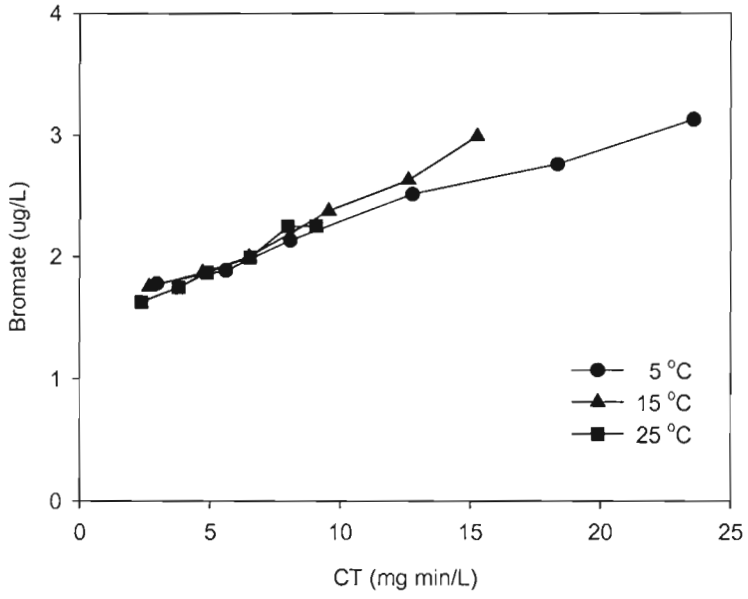

Figure 13. Bromate formation kinetics as a function of CT at different temperatures and pH 7.0

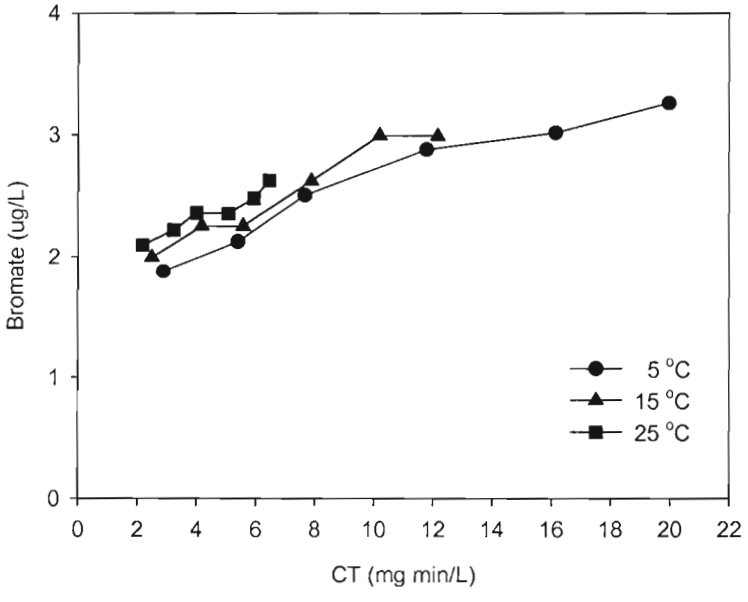

Figure 14. Bromate formation kinetics as a function of CT at different temperatures and pH 8.0

3.5 Numerical Simulations

Numerical simulations were carried out to predict the performance of the ozone contactor at the BWTP under a few design and operation scenarios. Of particular concern were residual ozone control and *C. parvum* oocyst inactivation, while formation of bromate received less attention since bromide concentration in raw water was relatively low as shown in Table 3. For all simulations, initial ozone concentration was assumed to be 1.0 mg/L, which would be maintained by ozone injector installed just before the ozone contactor. Table 7 summarizes the simulation scenarios studied. The values of pH (i.e., 6.0, 7.0, 8.0) and temperature (i.e., 5, 15, 25°C) used for simulations were the same as those used for batch tests. Dispersion numbers were varied from 0.1 and 10,000, which represent hydrodynamic conditions relatively close to PFR (d = 0.1) and those close to CSTR (d = 10,000), respectively. The contactor was divided into either 4 cells or 10 cells to simulate the effect of cell division.

Table 7. Simulation conditions for BWTP (Ansan, Korea).

Run ID	*pH*	*Temperature (°C)*	*Dispersion No.*	*No. of cells*
1	8.0	5, 15, 25	0.1	10
2	7.0	5, 15, 25	0.1	10
3	6.0	5, 15, 25	0.1	10
4	8.0	5, 15, 25	10,000	10
5	7.0	5, 15, 25	10,000	10
6	6.0	5, 15, 25	10,000	10
7	8.0	5, 15, 25	10,000	4
8	7.0	5, 15, 25	10,000	4
9	6.0	5, 15, 25	10,000	4

3.5.1. Residual Ozone Concentration

Controlling ozone concentration is a critical parameter for plant operation because any residual in effluent may negatively impact subsequent unit processes. For example, residual ozone might oxidize the surface of activated carbons in a following BAC filter. Therefore, quenching the ozone residual is often a necessary step.

pH effect

The simulation results suggest that the inlet ozone concentration of 1 mg/L might result in a relatively large ozone residual at the effluent of ozone contactor, which could be viewed problematic due to aforementioned reasons. This residual ozone concentration would be strongly affected by pH, with the highest value at pH 6.0 and the lowest at pH 8.0 among three pHs investigated as shown in Figure 15. Therefore, increasing the pH could be considered if decreasing ozone concentration at the effluent is desired without decreasing inlet ozone concentration below 1 mg/L. However, it should be noted that option of increasing pH above 8.0 should be carefully approached due to possible other complications especially in water distribution network.

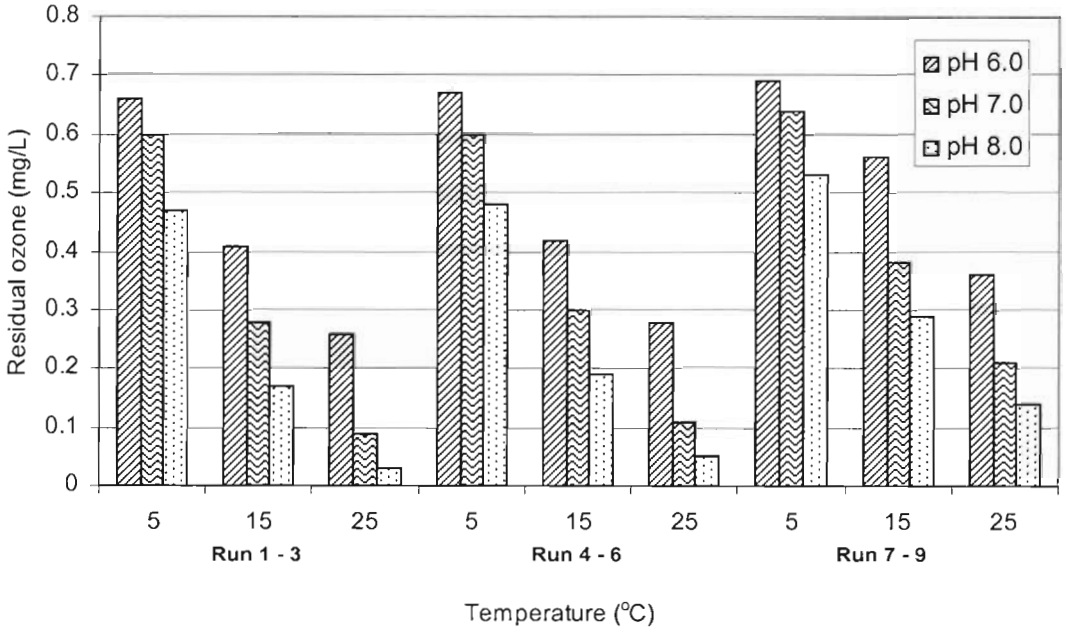

Figure 15. Residual ozone concentrations at the contactor effluent predicted for the Runs 1 through 9.

Temperature effect

Temperature is another important factor affecting residual ozone concentration. Figure 15 shows that residual ozone concentrations in the effluent would significantly decrease as temperature increases from 5 to 25°C. Note that predicted ozone concentration in the effluent was highest when the temperature was lowest at 5°C and pH was lowest at 8.0 for all design

scenarios. Therefore, controlling residual ozone below a critical concentration level should consider the combined effect of both temperature (i.e., during cold seasons) and pH.

Dispersion effect

Figure 15 shows that hydrodynamic conditions (i.e., degree of dispersion in ozone contactor) would exert a relatively small effect on residual ozone concentration. Note that simulation Runs 1-3 were performed with a dispersion number of 0.1 (i.e., close to PFR) and runs 4-5 with a dispersion number of 10,000 (i.e., close to CSTR), respectively. While the hydrodynamic conditions closer to PFR would result in less residual ozone concentration for all pHs and temperatures but the difference was relatively negligible compared to the effects of pH and temperature.

Number of Cells

Simulations were performed for Runs 4-6 with ten cells and Runs 7-9 with four cells dividing the ozone contactor. Note that Runs 4-9 were performed with the same dispersion number of 10,000. Therefore, having more cells results in the overall contactor hydrodynamic conditions closer to PFR. Simulation results suggested the effluent ozone concentration would be much lower for Runs 4-6 (i.e., 10 cells) than Run 7-9 (i.e., 4 cells) especially at 25°C. The difference became smaller at 5°C. This result suggests that dividing the ozone contactor into larger number of cells might be considered if reducing residual ozone concentration at the effluent becomes a concern.

Summary

Given 1 mg/L of ozone at the influent of ozone contactor, simulation results suggest that it might be challenging to remove the residual ozone at the contactor effluent unless addition of quenching agents such as hydrogen peroxide is considered. Presence of residual ozone will become more problematic as temperature and pH decrease. Hydrodynamic conditions might also play an important role especially with respect to division of the contactor using baffle walls.

3.5.2 *C. parvum* oocyst Inactivation

C. parvum oocyst inactivation is one of the primary objectives of ozonation process in many utilities including the BWTP. Effects of pH, temperature, dispersion, and cell division of ozone contactor on *C. parvum* oocyst inactivation efficiency were analyzed using the *OCM* software.

pH effect

Level of *C. parvum* oocyst inactivation is determined only by degree of exposure to residual ozone, often expressed in terms of CT. Since residual ozone concentration would be higher at lower pH as previously discussed, predicted *C. parvum* oocyst inactivation also increased as pH was decreased as shown in Figure 16.

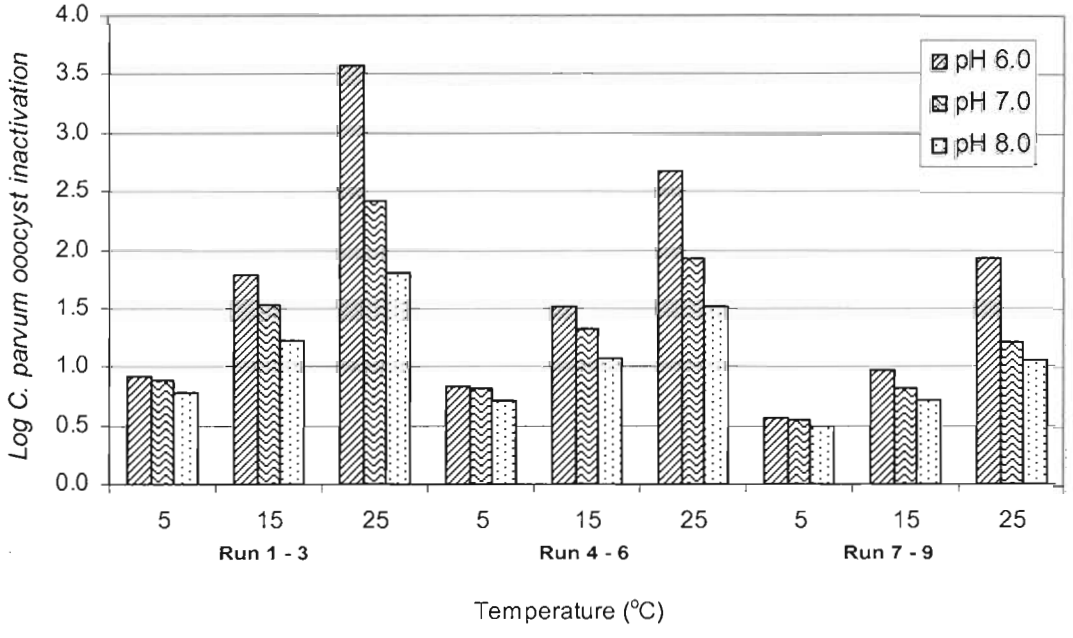

Figure 16. Log *C. parvum* oocyst inactivation at the contactor effluent predicted for the Runs 1 through 9.

Temperature effect

Kinetics of *C. parvum* oocyst inactivation are strongly affected by temperature. Accordingly, as temperature was decreased, predicted inactivation efficiency dramatically decreased for all Runs. It was noteworthy that the level of inactivation at 5°C could be as low as

0.5 log, which might raise concerns on effectiveness of ozone process at the BWTP especially during cold seasons.

Dispersion Effect

Figure 17 shows that effect of hydrodynamic conditions on *C. parvum* oocyst inactivation was more apparent that that on residual ozone concentration. Simulation Runs 1-3 and Runs 4-5 were performed with dispersion number of 0.1 and 10,000, respectively. Simulation results show that hydrodynamic condition close to PFR (d = 0.1) resulted in much higher level of inactivation for all pHs and temperatures than that close to CSTR (d = 10,000). This results, consistent with previous observations in the literature (Kim et al., 2002a, 2002b, 2004) suggest that designing a contactor hydrodynamic condition close to plug flow (i.e. smaller dispersion number) is favorable to achieve higher inactivation efficiency of *C. parvum* oocyst for the same amount of ozone input.

Number of Cells

As previously described, simulation Runs 4-6 were performed with ten cells and Run 7-9 with four cells. All the simulations were performed assuming the same dispersion number of 10,000. Predicted inactivation efficiency was much higher for Runs 7-9 than Runs 4-6. This results suggest that designing overall contactor hydrodynamic conditions closer to PFR by increasing the number of cell division might be beneficial to increase the inactivation efficiency when other conditions remain unchanged.

Summary

Increasing the number of cells in the ozone contactor and lowering back-mixing in each cell are recommended to increase the efficiency of *C. parvum* oocyst inactivation, . Low pH is favorable for achieving higher inactivation efficiency due to increase in residual ozone concentration. However, if minimizing residual ozone at the contactor effluent becomes a concern, pH of ozone contactor influent should be carefully optimized. Achieving adequate level of *C. parvum* oocyst inactivation at lower temperatures might be challenging for this specific ozone contactor.

3.5.3 Bromate Formation

Simulation results suggest that bromate would be formed rapidly at the initial stage of ozonation for all the scenarios investigated, consistent with the observation at the batch tests. However, predicted overall effluent bromate concentrations were less than 3 μg/L, which is much lower than the current MCL of 10 μg/L imposed by the USEPA. These results suggest that bromate formation during ozonation might not be a concern for the ozone contactor at the BWTP.

3.5.4 Simulation Results For Each Scenarios

This section shows the details of results obtained for all the simulation runs performed for this study including the profiles of ozone concentration, *C. parvum* oocyst inactivation, and bromate concentration throughout the ozone contactor as well as values of these entities at the contactor effluent.

Run 1 (pH 8.0, d=0.1, 10cells)

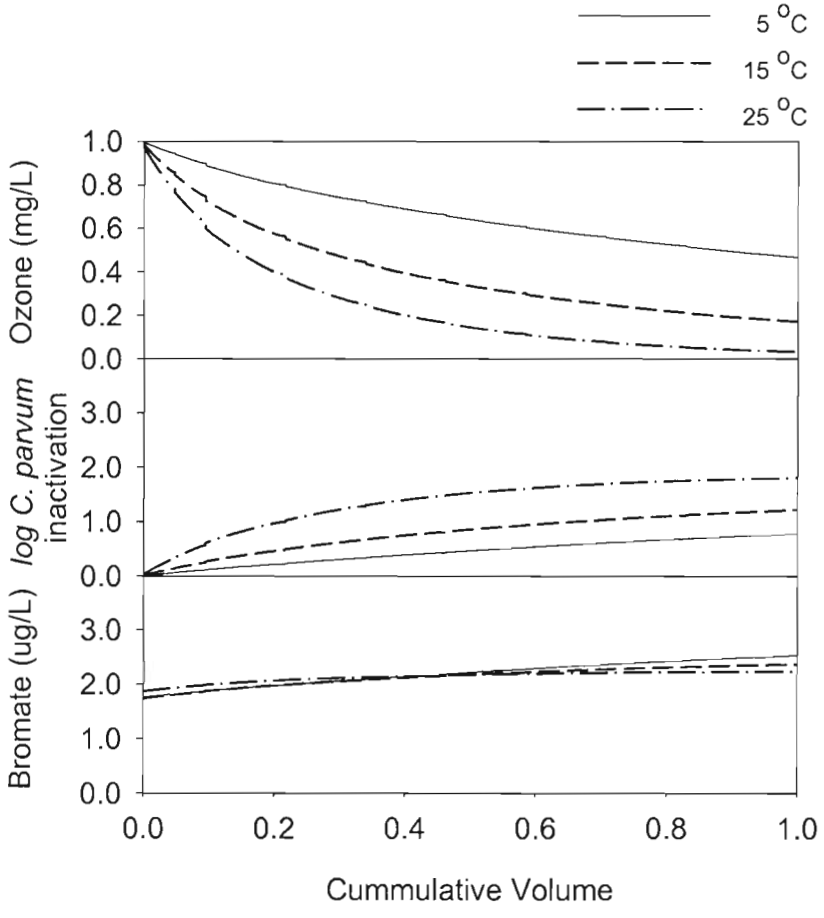

Figure 17. Simulation results of Run 1 (pH 8.0, d=0.1, 10 cells).

Table 8. Simulated results for ozone contactor final effluents at pH 8.0; d=0.1; 10 cells.

	Ozone (mg/l)	Log. *C. parvum* inactivation	Bromate (μg/L)
5 °C	0.47	0.78	2.53
15 °C	0.17	1.22	2.37
25 °C	0.03	1.81	2.24

Run 2 (pH 7.0, d=0.1, 10cells)

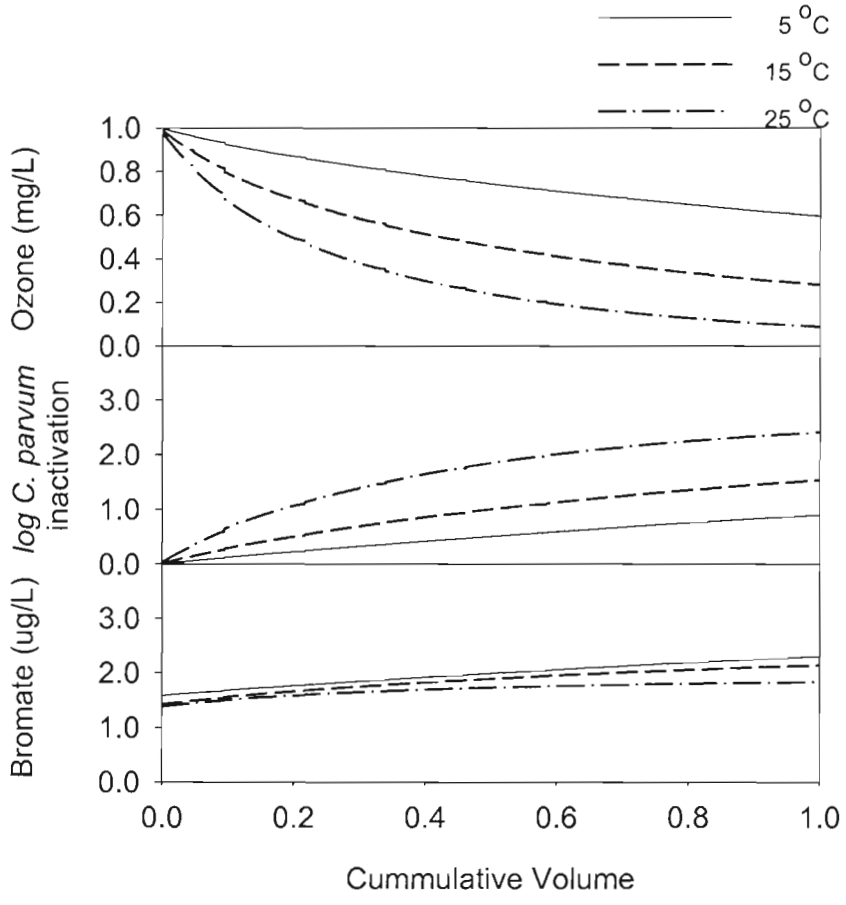

Figure 18. Simulation results of Run 2 (pH 7.0, d=0.1, 10 cells).

Table 9. Simulated results for ozone contactor final effluents at pH 7.0; d=0.1; 10 cells.

	Ozone (mg/l)	Log. *C. parvum* inactivation	Bromate (μg/L)
5 °C	0.60	0.89	2.30
15 °C	0.28	1.53	2.14
25 °C	0.09	2.41	1.83

Run 3 (pH 6.0, d=0.1, 10cells)

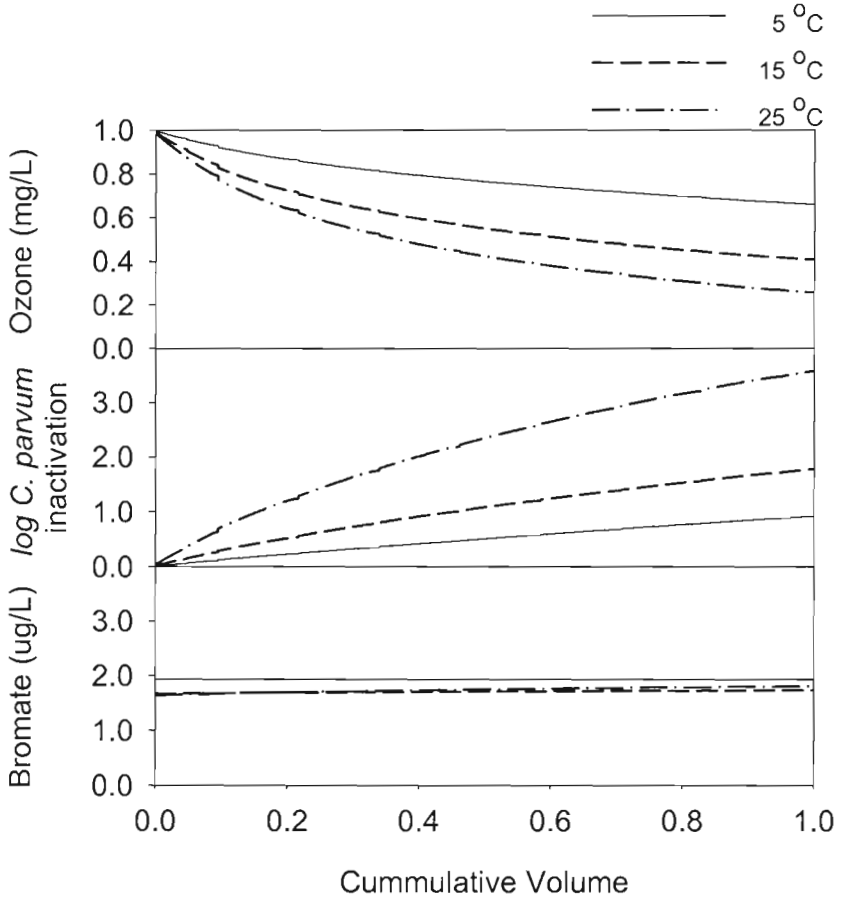

Figure 19. Simulation results of Run 3 (pH 6.0, d=0.1, 10 cells).

Table 10. Simulated results for ozone contactor final effluents at pH 6.0; d=0.1; 10 cells.

	Ozone (mg/l)	Log. *C. parvum* inactivation	Bromate (μg/L)
5 °C	0.66	0.92	1.94
15 °C	0.41	1.78	1.74
25 °C	0.26	3.58	1.81

Run 4 (pH 8.0, d=10,000, 10cells)

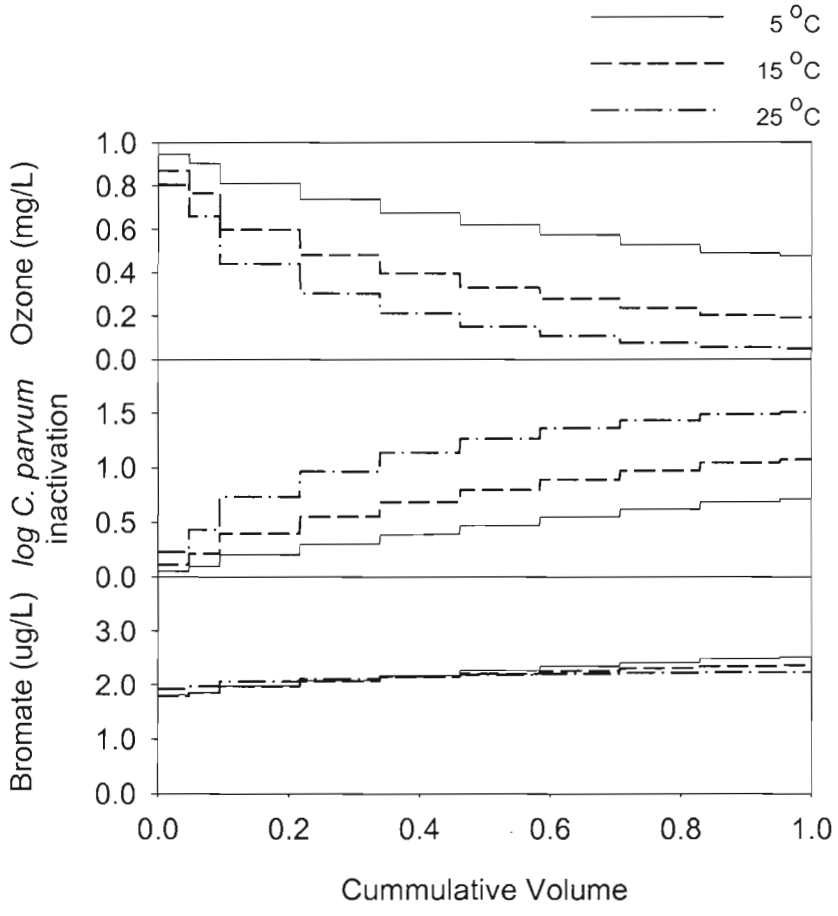

Figure 20. Simulation results of Run 4 (pH 8.0, d=10,000, 10 cells).

Table 11. Simulated results for ozone contactor final effluents at pH 8.0; d=10,000; 10 cells.

	Ozone (mg/l)	Log. *C. parvum* inactivation	Bromate (μg/L)
5 °C	0.48	0.71	2.51
15 °C	0.19	1.07	2.36
25 °C	0.05	1.51	2.24

Run 5 (pH 7.0, d=10,000, 10cells)

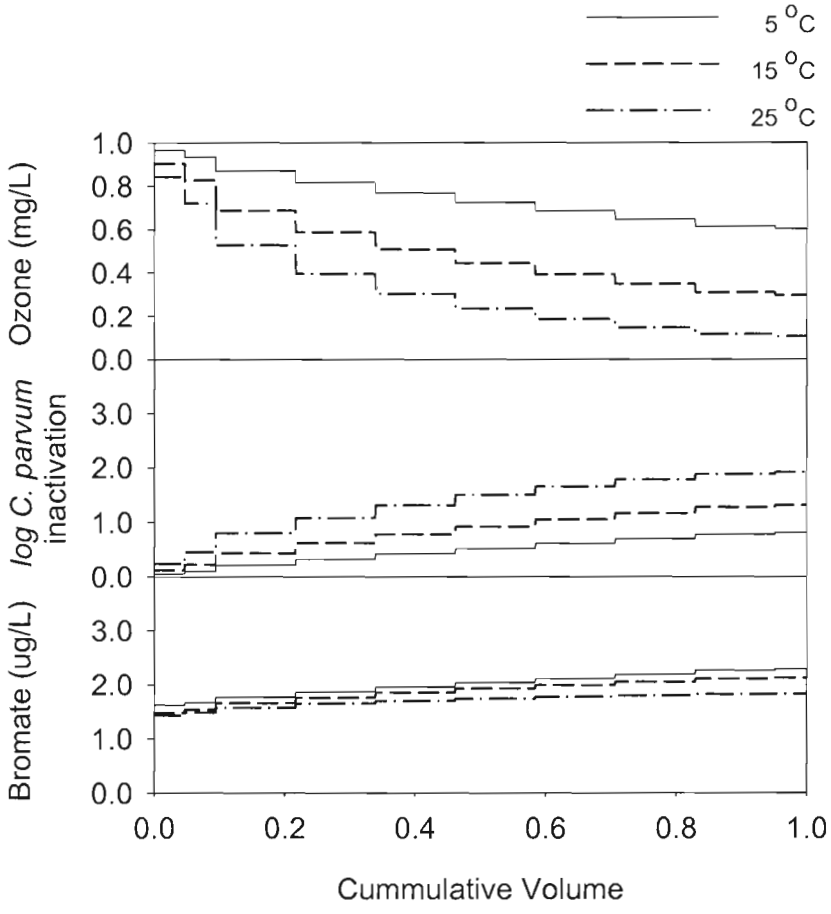

Figure 21. Simulation results of Run 5 (pH 7.0, d=10,000, 10 cells).

Table 12. Simulated results for ozone contactor final effluents at pH 7.0; d=10,000; 10 cells.

	Ozone (mg/l)	Log. *C. parvum* inactivation	Bromate (μg/L)
5 °C	0.60	0.81	2.29
15 °C	0.30	1.32	2.13
25 °C	0.11	1.92	1.83

Run 6 (pH 6.0, d=10,000, 10cells)

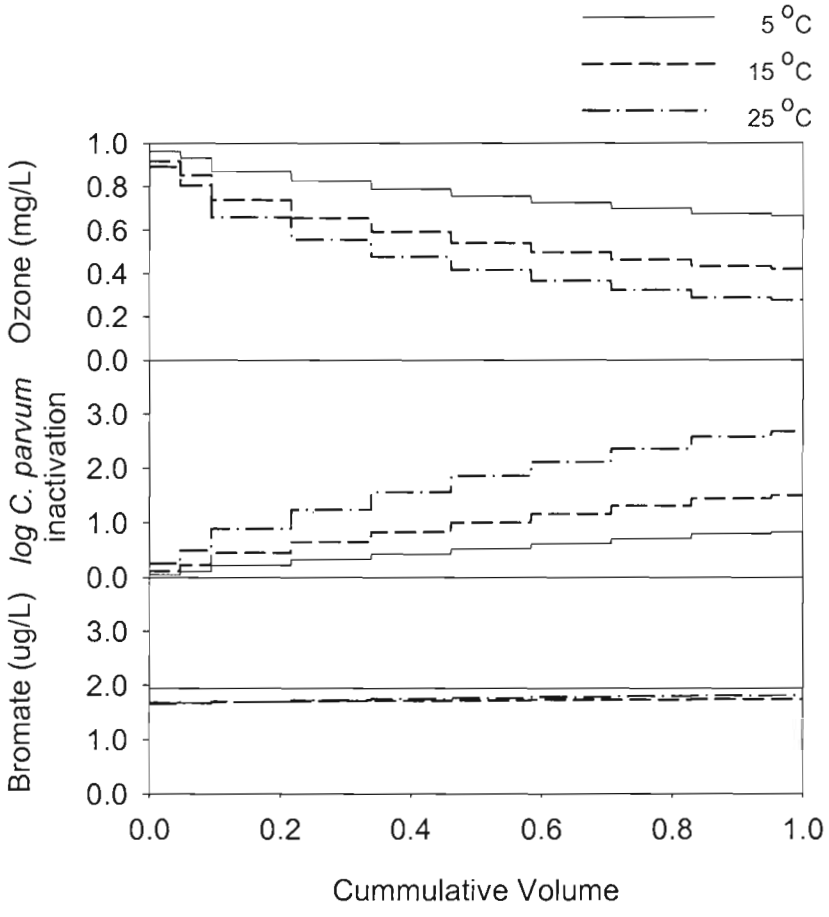

Figure 22. Simulation results of Run 6 (pH 6.0, d=10,000, 10 cells).

Table 13. Simulated results for ozone contactor final effluents at pH 6.0; d=10,000; 10 cells.

	Ozone (mg/l)	Log. *C. parvum* inactivation	Bromate (μg/L)
5 °C	0.67	0.83	1.94
15 °C	0.42	1.51	1.74
25 °C	0.28	2.68	1.81

Run 7 (pH 8.0, d=10,000, 4 cells)

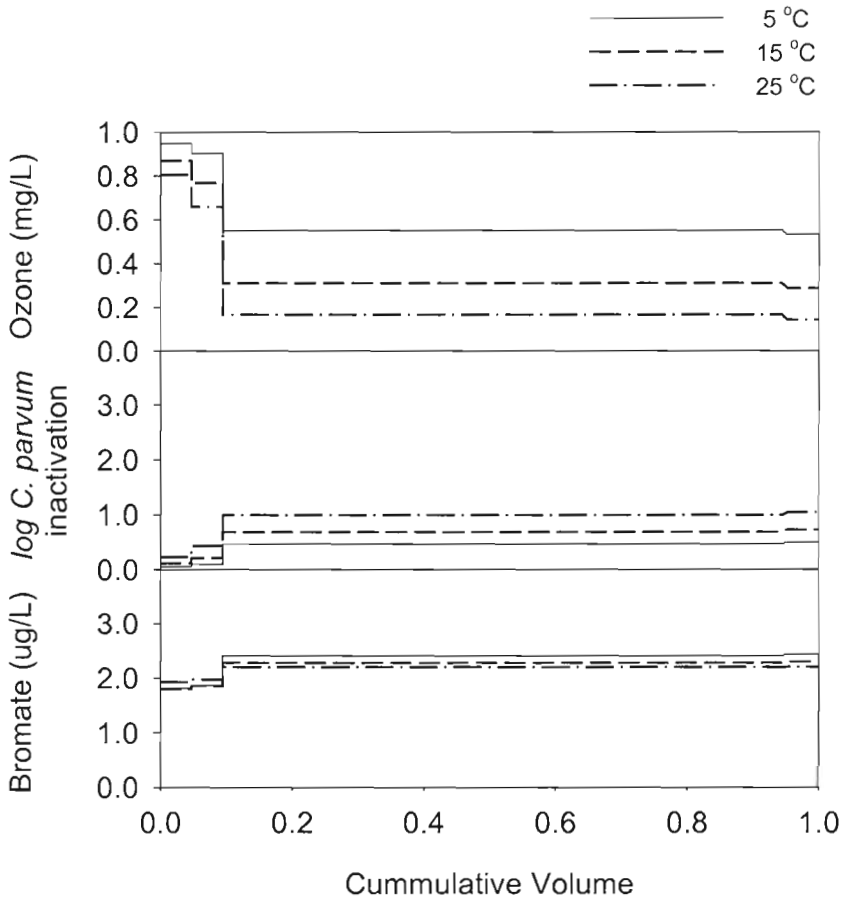

Figure 23. Simulation results of Run 7 (pH 8.0, d=10,000, 4cells).

Table 14. Simulated results for ozone contactor final effluents at pH 8.0; d=10,000; 4 cells.

	Ozone (mg/l)	Log. *C. parvum* inactivation	Bromate (μg/L)
5 °C	0.53	0.49	2.43
15 °C	0.29	0.72	2.30
25 °C	0.14	1.05	2.21

Run 8 (pH 7.0, d=10,000, 4 cells)

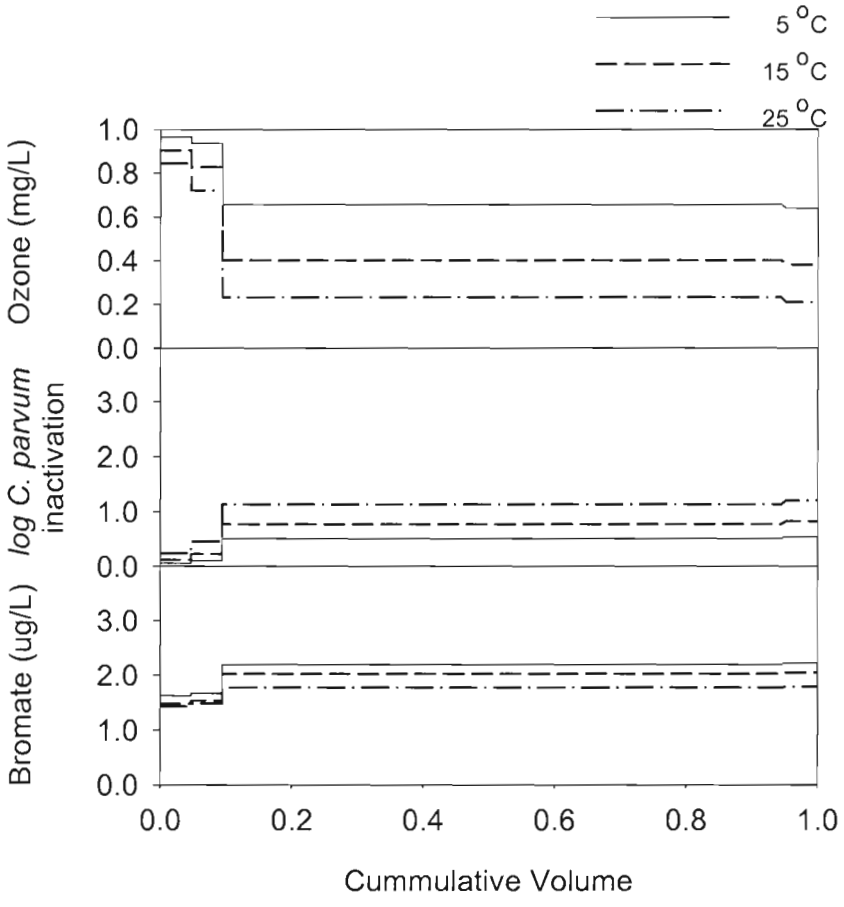

Figure 24. Simulation results of Run 8 (pH 7.0, d=10,000, 4cells).

Table 15. Simulated results for ozone contactor final effluents at pH 7.0; d=10,000; 4 cells.

	Ozone (mg/l)	Log. *C. parvum* inactivation	Bromate (μg/L)
5 °C	0.64	0.54	2.22
15 °C	0.38	0.82	2.05
25 °C	0.21	1.21	1.79

Run 9 (pH 6.0, d=10,000, 4 cells)

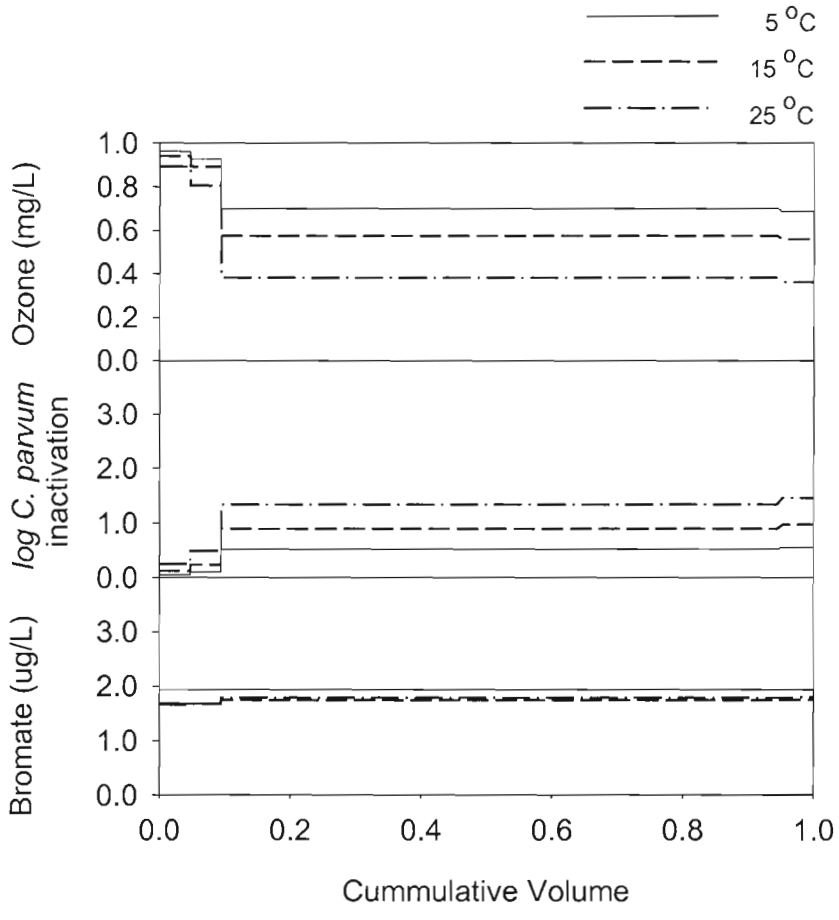

Figure 25. Simulation results of Run 9 (pH 6.0, d=10,000, 4cells).

Table 16. Simulated results for ozone contactor final effluents at pH 6.0; d=10,000; 4 cells.

	Ozone (mg/l)	Log. *C. parvum* inactivation	Bromate (μg/L)
5 °C	0.69	0.56	1.93
15 °C	0.56	0.97	1.75
25 °C	0.36	1.46	1.80

4. CONCLUSIONS

Kinetics of ozone decay and bromate formation in the source water collected from the BWTP were determined from batch experiments using the MC-SFR system at different pHs and temperatures. These kinetics were used by the *OCM* software to predict the concentrations of ozone and bromate in the full-scale ozone contactor at the BWTP. Full-scale simulation performed using the *OCM* software suggested the followings:

1) Residual ozone concentrations in the contactor effluent would be greatly affected by changes in pH and temperature. Minimizing the residual ozone concentration at the effluent might become challenging when pH and temperature are decreased, unless inlet ozone concentration is reduced or a quenching agent is introduced.

2) Efficiency of *C. parvum* oocyst inactivation would be strongly affected by pH. It is noteworthy that adequate control of *C. parvum* oocyst might become significantly challenging especially when temperature is decreased. Designing the overall reactor hydrodynamic conditions closer to PFR by dividing the contactor into more cells and reducing backmixing in each cell might be desirable to achieve higher inactivation efficiency.

3) Predicted bromate concentration in the contactor effluent was relatively low. Therefore, as long as bromide level does not change significantly over time, bromate formation should not raise a concern for the ozonation process at the BWTP.

5. REFERENCES

Chen, C. M. (1998). "Modeling drinking water disinfection in ozone bubble-diffuser contactors." *Ph.D. Dissertation*, Purdue University, West Lafayette, Indiana.

Clark, R. M., Sivagenesan, M., Rice, E. W., Chen, J. (2002). "Development of a *Ct* Equation for the inactivation of *Cryptosporidium* oocysts with ozone." *Water Research*, 36(12), 3141-3149.

Dai, X.; Raymond, M. H. (2002). "Effect of NOM and biofilm on the removal of C. parvum oocysts in rapid filters.", *Water Research*, 36, 3523-3532

Driedger, A.; Staub, E.; Pinkernell, U.; Mariñas, B.; Köster, W.; von Gunten. U. (2001). "Inactivation of bacillus Subtilis spores and formation of bromate during ozonation.", *Water Research*, 35(12) pp2950-2960.

Driedger, A.M.; Rennecker, J.L.; Mariñas, B.J. (2000). "Sequential inactivation of *Cryptosporidium parvum* oocysts with ozone and free chlorine." *Water Research*, 34(14), 3591-3597

Driedger, A.M.; Rennecker, J.L.; Mariñas, B.J. (2001). "Inactivation of *Cryptosporidium parvum* oocysts with ozone and monochloramine at low temperature." *Water Research*, 35(1), 41-48

Elovitz, M. S.; von Gunten, U. (1999). "Hydroxyl Radical/Ozone Ratios During Ozonation Processes. I. The R_{ct} Concepts." *Ozone Science and Engineering*, 21(3), 239-260

Emelko, M. B. (2003). "Removal of viable and inactivated C. parvum by dual and tri media filtration.", *Water Research*, 37, 2998-3008

European Union. Amtsblatt der Europäischen Gemeinschaften. Richtlinie 98/83/EG des Rates. 3-12-1998, 1998, 32-54

Federal Register. National Primary Drinking Water Regulations; Disinfectants and Disinfection Byproducts; Final Rule. 1998, 63(241), 69389

Gyürék, L.; Finch, G.R.; Belosevic M. (1997). "Modeling chlorine inactivation requirements of *Cryptosporidium parvum* oocysts." *ASCE Journal of Environmental Engineering*, 123(9), 865-875

Gyürék, L.; Li, H.; Belosevic, M.; Finch, G.R. (1999). "Ozone inactivation kinetics of *Cryptosporidium* in phosphate buffer." *ASCE Journal of Environmental Engineering,* 125 (10), 913-924

Kim, D.; Kim, J. H. (2004). "Real-Time Monitor and Control of Ozone Disinfection Process." *International Ozone Association – Pan American Group Regional Conference*, Windsor, Ontario.

Kim, D.; Tang, G.; Haidri, S.; Mariñas, B. J. Couillard, L.; Shukairy, H. M; Kim, J. H. (2005b). "Simultaneous Simulation of Pathogen Inactivation and Bromate Formation in a Full-Scale Ozone Contactor by Computer Software." *Journal American Water Works Association* (in preparation).

Kim, J. H.; Elovitz, M. S.; von Gunten, U.; Shukairy, H. M.; Mariñas, B. J. (2005a). "Modeling *Cryptosporidium parvum* Inactivation and Bromate Formation during Ozone Disinfection of Natural Water in a Flow-through Ozone Contactor." *Environmental Science and Technology* (submitted)

Kim, J. H.; Tomiak, R. B.; Rennecker, J. L; Mariñas, B. J; Miltner, R. J; Owens, J. H. (2002b). "Inactivation of *Cryptosporidium* in a Pilot-Scale Ozone Bubble-Diffuser Contactor. Part I I:

Model Verification and Application." *ASCE Journal of Environmental Engineering*, 128(6), 522-532

Kim, J. H.; Tomiak, R. B; Mariñas, B. J. (2002a). "Inactivation of *Cryptosporidium* in a Pilot-Scale Ozone Bubble-Diffuser Contactor. Part I : Model Development." *ASCE Journal of Environmental Engineering*, 128(6), 514-521

Kim, J.H.; von Gunten, U.; Mariñas, B. J. (2004). "Modeling Bromate Formation and *Cryptosporidium parvum* Inactivation in Synthetic Waters." *Environmental Science and Technology*, 38, 2232-2241

Korich, D. G.; Mead, J. R.; Madore, M. S.; Sinclair, N. A.; Sterling, C. R.(1990). Effect of ozone, chlorine dioxide, chlorine, monochloramine on C. parvum oocyst viability, *Appl Environ. Microbiol.*, 56, 1423-1428

Langlais, B.; Reckhow, D. A.; Brink, D. R. (1991). "Ozone in water treatment: Application and engineering.", Lewis Publishers

Lev, O., and Regli, S. (1992a). "Evaluation of ozone disinfection systems: characteristic time T." *ASCE Journal of Environmental Engineering*, 118(2), 268-285.

Mariñas B. J., Liang, S., and Aieta, M. E. (1993). "Modeling hydrodynamics and ozone residual distribution in a pilot-scale ozone bubble-diffuser contactor." *Journal of American Water Works Association*, 85(3), 90-99.

Pinkernell, U.; von Gunten, U. (2001). "Bromate Minimization during Ozonation: Mechanistic Considerations." *Environmental Science and Technology*, 35(12), 2525-2531

Rennecker, J. L., Mariñas B. J., Rice E. W., and Owens J. H. (1999). "Inactivation of *Cryptosporidium parvum* oocyst with ozone." *Water Research,* 33(9), 2481-2488.

Rennecker, J. L.; Driedger, A. M.; Rubin, S. A.; Mariñas, B. J. (2000). Synergy in sequential inactivation of C. parvum with ozone/free chlorine and ozone/monochloramine." *Water Research,* 34(17), 4121-4130

Rennecker, J. L.; Kim, J. H.; Corona-Vasquez, B.; Mariñas, B. J. (2001). Role of disinfectant concentration and pH in the inactivation kinetics of C. parvum oocysts with ozone and monochloramine., *Environmental Science and Technology*, 35(13), 2752-2757

Rennecker, J. L.; Mariñas B. J.; Rice E. W.; Owens J. H. (1999). "Inactivation of *Cryptosporidium parvum* Oocyst with Ozone." *Water Research,* 33(9), 2481-2488

Rennecker, J.L.; Driedger, A.M.; Rubin, S.A.; Mariñas, B.J. (2000). "Synergy in Sequential Inactivation of *Cryptosporidium parvum* with Ozone/Free Chlorine and Ozone/Monochloramine." *Water Research*, 34(17), 4121-4130

Ribas, F.; Bernal, A.; Perramón, J. (2000). "Elimination of Giardia cysts, Cryptosporidium oocysts, turbidity and particles in a drinking water treatment plant with clarification and double filtration.", *Water Science and Technology*, 41(7), 203-211

Siddiqui, M.S. and Amy, G.L. (1993). "Factors affecting DBP formation during ozone-bromide reactions.", *J. AWWA*, 85(1), pp63-72

Smith, V. (1995). "Complacency caused Milwaukee's crypto outbreak", *J. AWWA*, 75(1), 8-10

Tang, G.; Adu-Sarkodie, K.; Kim, D.; Kim, J-. H., Teefy, S.; Shukairy, H. M.; Mariñas, B. J. (2005). "Modeling *Cryptosporidium Parvum* Oocyst Inactivation and Bromate Formation in a Full-Scale Ozone Contactor.", *Environmental Science and Technology* (Submitted)

United States Environmental Protection Agency. *Stage 2 Occurrence Assessment for Disinfectants and Disinfection Byproducts*. EPA 68-C-99-206, Washington, DC, 2003.

Van der Kooji, D. (1992). "Assimilable organic carbon as an indicator of bacterial regrowth.", J. *AWWA*, Feb., 57-65

Volk, C. J., Lechevallier, M. W. (2002). "Effects of conventional treatment on AOC and BDOC levels.", *J. AWWA*, June, 94(6), 112-123

Von Gunten, U.; Hoigné, J. (1994). "Bromate formation during ozonation of bromide containing waters: Interaction of ozone and hydroxyl radical reactions.", *Environmental Science and Technology*, 28, 1234-1242

Westerhoff, P.; Song, P.; Amy, G.; Minear, R. (1998). "Numerical kinetic models for bromide oxidation to bromide and bromate.", *Water Research*, 32(5), 1687-1699